

Micromachined silicon force sensor based on diffractive optical encoders for characterization of microinjection

X.J. Zhang^{a,*}, S. Zappe^a, R.W. Bernstein^b, O. Sahin^a, C.-C. Chen^a,
M. Fish^c, M.P. Scott^c, O. Solgaard^a

^a Department of Electrical Engineering, Stanford University, Stanford, CA 94305, USA

^b Department of Microsystems, SINTEF Electronics & Cybernetics, Oslo, Norway

^c Department of Developmental Biology, School of Medicine, Stanford University, Stanford, CA 94305, USA

Received 11 November 2003; accepted 21 November 2003

Available online 22 January 2004

Abstract

We present a micrograting-based force sensor integrated with a surface micromachined silicon-nitride probe for penetration and injection into *Drosophila* embryos. The probe is supported by springs of a known spring constant, and the penetration force is determined from displacement measurements using a high-resolution, miniaturized optical encoder that is designed to only be sensitive to axial deflections of the probe. The optical-encoder force sensor exhibits configurable sensitivity and dynamic range, allowing monitoring over a wide range of forces. The periodicity of the encoder response can be used for calibration of the injector displacement and to obtain information about the localized elastic properties of the target. We used a force sensor with a measured spring constant of 1.85 N/m for penetration experiments on *Drosophila* embryos, and found a penetration force of 52.5 μN ($\pm 13.2\%$) and a membrane displacement of 58 μm ($\pm 5.2\%$).

© 2003 Elsevier B.V. All rights reserved.

Keywords: Force sensor; MEMS optical encoder; Microinjection; *Drosophila* embryo

1. Introduction

Localized and accurate microinjection of genetic material into biological model systems, such as *Drosophila*, will enable a variety of studies of developmental biology and genetics [1]. For such studies to be carried out *in vivo*, the damage caused by the injection must be minimized. We have developed surface micromachined silicon-nitride injectors [2] with integrated force sensors for measurements of the penetration force and needle–membrane interactions under various physiological conditions.

The force sensor is an optical encoder based on transmission phase gratings integrated with the injector. Precise displacement measurements using diffractive gratings is an established technology [3], and optical encoders have been developed for precise measurements of displacement and revolution angle for a variety of applications. However, the large size and expensive manufacturing of conventional encoders make them unsuitable as integrated sensing devices. Recently, there has been significant renewed interest in using diffractive micro-optical elements as displacement sensors

in atomic force microscopes (AFM) [4], MEMS capacitive ultrasonic transducers [5] and accelerometers with nano-g resolution [6]. For optical encoders, Sawada et al. demonstrated a hybrid integrated encoder with a single grating on silicon [7]. Hane et al. designed a dual-grating miniaturized displacement sensor using grating imaging [8]. These advancements in microfabricated diffractive grating optics enable integrated optical encoders for sensing and microscopy of embryos and single cells.

2. Operational principles and design

As shown in Fig. 1, the force encoder consists of two identical constant-period transmission phase gratings that are vertically aligned when no force is applied. Phase gratings are used because they have higher optical diffraction efficiency than amplitude gratings [9]. When a force is applied to the injector (not shown in Fig. 1) in the x -direction, the upper index grating is displaced with respect to the bottom grating. This changes the diffraction efficiency of the phase grating, and the relative position of the two gratings can be determined by the intensities in the diffraction orders. The diffraction characteristics of the dual transmission

* Corresponding author. Tel.: +1-408-421-9632; fax: +1-650-725-7509.
E-mail address: xjzhang@stanfordalumni.org (X.J. Zhang).

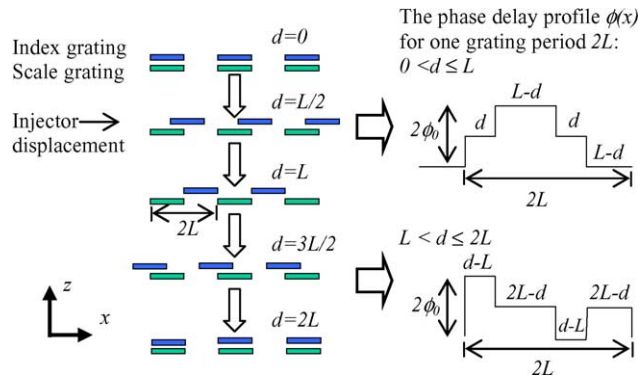


Fig. 1. Principle of the injection-force encoder: $2L$ is the period of the grating with 50% duty cycle; $d = \text{mod}(x, 2L)$ is the displacement of the microinjector modulus $2L$; ϕ_0 represents a relative phase delay over the thickness of one grating finger.

phase grating can be analyzed by Fraunhofer diffraction theory. The first diffraction mode intensity $I_1(d)$ is a periodic function of injector displacement:

$$I_1(d) = I_0 N^2 \left(\frac{\sin^2 c^2(Nd/2L)}{\sin^2 c^2(d/2L)} \right) \left[(L-d) \sin c \left(\frac{L-d}{4L} \right) \right]^2 \times \sin^2 \phi_0 G(d) \quad (1)$$

$$G(d) = \begin{cases} \sin^2 \frac{\pi(L+d)}{4L} & d \in [0, L] \\ \sin^2 \frac{\pi(3L-d)}{4L} & d \in [L, 2L] \end{cases} \quad (2)$$

where I_0 is the illuminating light intensity, N the number of grating periods under illumination, $\phi_0(x) = (2\pi/\lambda)(n_1 - n_0)t$ is the phase delay over the thickness of one grating finger, $2L$ the period of the grating, d the displacement of the injector modulus $2L$. We define the force-sensor sensitivity as the change in the intensity of the first diffraction mode with respect to a unit displacement of the upper grating. The dynamic range is defined as the total range of motion over which the position can be unambiguously determined from the diffraction pattern. From Eq. (1) we see that the sensitivity and dynamic range of the sensor can be tuned by changing the number of grating fingers, N , that are illuminated and/or by changing the grating period, $2L$.

The encoder is designed to be sensitive to translation in the x -direction, while the sensitivities to the other 5 degrees of freedom of motion are minimized. Translation in the y -direction can be neglected because it is small ($k_y \gg k_x$) and has little effect on the optical readout. Likewise, rotation about the x and y axes do not affect the diffraction of the gratings and can therefore be ignored. Motion in the z -direction is also inconsequential, because the weak reflections from the grating elements lead to only small variations of the phase shift through the encoder as a function of the separation of the gratings in the z -direction. To ensure weak reflections, the grating elements must be designed such that the fields reflected from their fronts and backs

interfere destructively. We achieve destructive interference by using grating made of silicon nitride with a refractive index of $n_1 \approx 1.9$ and a thickness of $t = 1.5 \mu\text{m}$. Thus the phase shift $(4\pi/\lambda)n_1 t$ associated with traversing the grating film twice is approximately an integer multiple of 2π at HeNe wavelength $\lambda = 633 \text{ nm}$. Combined with the π phase shift of the internal reflection at the nitride/air interface, this leads to destructive interference of the two parts of the reflected field, and therefore the reflection from the grating elements is minimized. Accurate control of the film thickness can be achieved by monitored etch-back after film deposition. Silicon nitride is well suited for our gratings, because its index allows us to minimize the back reflections and at the same time achieve a relatively high value (~ 0.5) for the factor $\sin^2(\phi_0)$ that determines the diffraction efficiency (see Eq. (1)). The remaining degree of freedom of motion is rotation about the z -axis. The encoder is sensitive to such rotation, so it must be minimized. The encoder therefore has maximally separated, straight suspensions to create a large spring constant for rotation about the z -axis.

Fig. 2 illustrates the trade-off between sensitivity and dynamic range. Encoders with a larger grating period have a larger dynamic range, but low sensitivity (dotted line), while the opposite is true for encoders with a finer pitch (solid line). For a given period, the sensitivity can be improved by increasing the number of grating periods that are illuminated, again at the cost of a reduced range (dash-dotted line). We can therefore use two gratings, or one grating with two different illumination conditions, to create a sensor with high sensitivity and high dynamic range. The periodicity of the encoder response can also be used to calibrate the relative displacement of the gratings. This is useful in measurements where the injector is interacting with a compliant structure.

The accuracy of the force measurements depends on the spring constant of the movable index grating structure. The

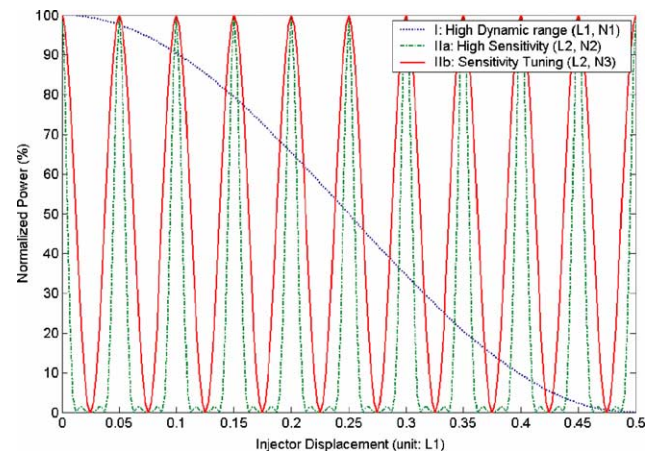


Fig. 2. Tuning of force encoder's sensitivity and dynamic range by: (I) increasing half-grating pitch period $L = L_1$ for high dynamic range; (II) varying number of grating fingers $N = (N_2, N_3)$ for given L for local high sensitivity enhancement within $2L$ injector displacement ($L_1 = 20L_2$, $N_2 = 4N_{1,3}$).

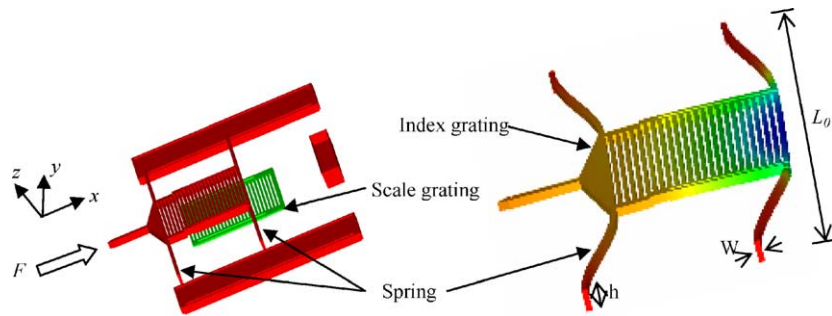


Fig. 3. Solid models for optical-encoder force sensor at static state (left) and the deformation of the supporting beams under central load on the force probe integrated with the index micro-grating (right).

Table 1
Optical-encoder force-sensor design parameters^a

Index micro-grating	
Period, $2L$ (μm)	20 (10, 30)
Thickness, h (μm)	1.5
Supporting beam (spring)	
Thickness, h (μm)	1.5
Length, L_0 (μm)	850
Width, W (μm)	8, 15, 30
Spring constant (N/m)	2.2, 14.5, 115.2
Resonant frequency (kHz)	13.9, 35.8, 100.8

^a Spring constants and resonant frequencies are simulated for a laterally loaded spring structure (see Fig. 3) with beam width $W = 8, 15,$ and $30 \mu\text{m}$, thickness $h = 1.5 \mu\text{m}$ and probe with length $L_0 = 80 \mu\text{m}$, and tip sidewall area $S = 10 \mu\text{m}^2$ and $\theta = 60^\circ$.

spring constants were simulated for the geometry shown in Fig. 3. A one-dimensional elastic model was used for the doubly supported beam. For a center-loaded doubly clamped beam, the relation between the applied force F and the deflection along x -direction is composed of both linear and

non-linear terms. The small-deflection linear bending term is proportional to the beam moment of inertia hW^3 , while the non-linear stretching term is proportional to hW , so thicker beams have more linear characteristics than thinner beams. For our force sensor, the transition from bending-dominated behavior to stretching-dominated behavior occurs when the deflection is about $10W$. Thus for our penetration experiments, the sensor is expected to operate mainly in the linear range. With normally applied pressure over the two sidewalls of the probe tip, the stress and displacement vector distribution across the device were simulated using the finite element method (FEM) for supporting beams of width 8, 15 and $30 \mu\text{m}$. The calculated spring constants and resonant frequencies are listed in Table 1.

3. Fabrication process

As shown in Fig. 4, the fabrication starts with the deposition and patterning of a $0.5 \mu\text{m}$ silicon-nitride layer

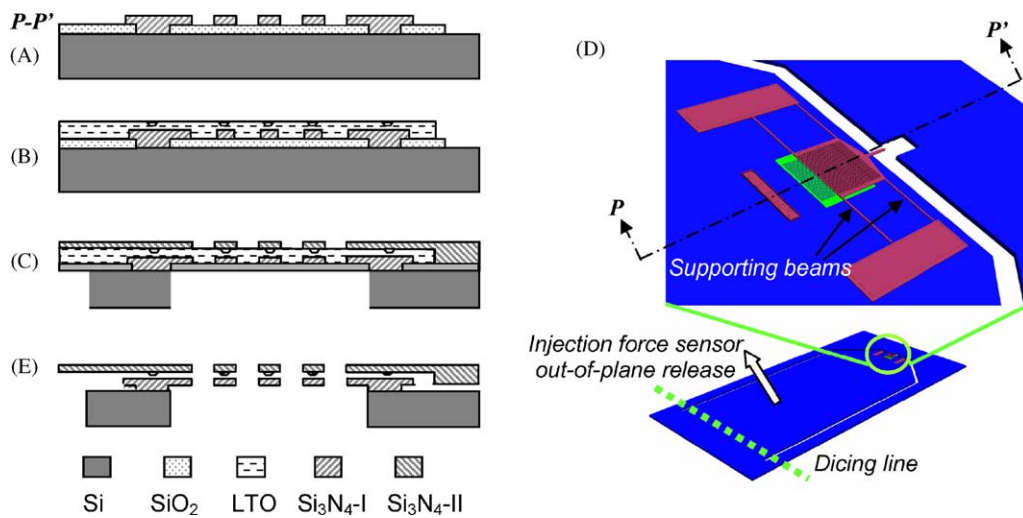


Fig. 4. Fabrication process of the optical-encoder injection force sensor: (A) deposition and patterning of a $0.5 \mu\text{m}$ silicon-nitride layer on top of low temperature oxide layer to form the fixed scale grating; (B) deposition of a $2 \mu\text{m}$ sacrificial oxide for releasing the upper index grating with an array of anti-sticking dimples formed by oxygen-plasma etching; (C) deposition and patterning a second $1.5 \mu\text{m}$ silicon-nitride layer to form the upper index grating, and deep reactive ion etch of the backside to form the optical interconnects for illuminating the gratings; (D) release of the injector with the force sensor from the wafer along the dicing line; (E) the upper grating with the probe is released using buffered HF solution, and critical point drying is performed to avoid unintended adhesion of the released structure to the substrate.

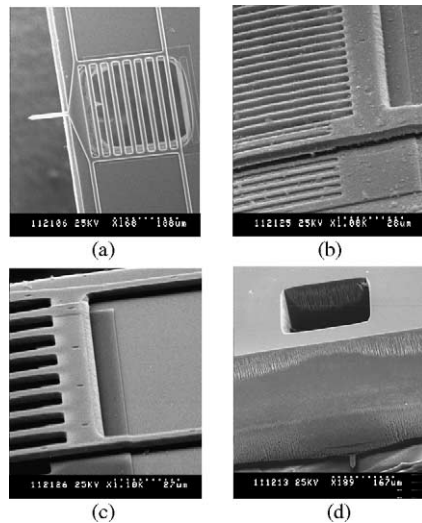


Fig. 5. SEM of: (a) optical-encoder force sensor; (b) index and scale gratings with $20\ \mu\text{m}$ pitch and $2\ \mu\text{m}$ vertical gap; (c) junction between the gratings and the supporting beams, with embedded anti-sticking dimples; (d) backside DRIE-ed optical illuminating aperture, with microinjector appearing on the other side.

on the oxidized silicon wafer to form the fixed scale grating ($10\text{--}30\ \mu\text{m}$ periods). Then $2\ \mu\text{m}$ low temperature oxide (LTO) is deposited as the sacrificial layer to allow release of the upper index grating with the integrated injector. A second $1.5\ \mu\text{m}$ silicon-nitride layer is deposited and patterned to form the upper index grating, and an array of anti-sticking dimples is formed by oxygen-plasma etching of the LTO before deposition of the second nitride layer. The injection force characterizations presented in this paper were acquired using optical encoders with probes without hollow channels, but integrated hollow injectors can be realized by embedding sacrificial LTO layer between the two silicon-nitride films of the probe. A deep reactive ion etch (DRIE) step is performed on the backside of the wafer to form the optical interconnect for illuminating the gratings. Finally, the force-sensor chip is removed from the wafer and released using buffered HF followed by critical point drying (CPD) to avoid unintended adhesion of the released structure to the substrate. Fig. 5 shows scanning electron micrographs (SEMs) of the injector with the integrated optical-encoder force sensor.

We selected silicon nitride (Si_3N_4) as the grating material due to the need for stress-optimized thin films of good optical quality. The optical transmission of $1.5\ \mu\text{m}$ thick silicon nitride, deposited under NH_3 -rich conditions, was measured to be approximately 83% at 633 nm. The gratings therefore only have weak amplitude modulation, and the transmission encoder can be considered to consist of pure phase gratings.

4. Results and discussion

For DC calibration of the force sensor, we used a SINTEF[®] piezoresistive microscale with a sensitivity of

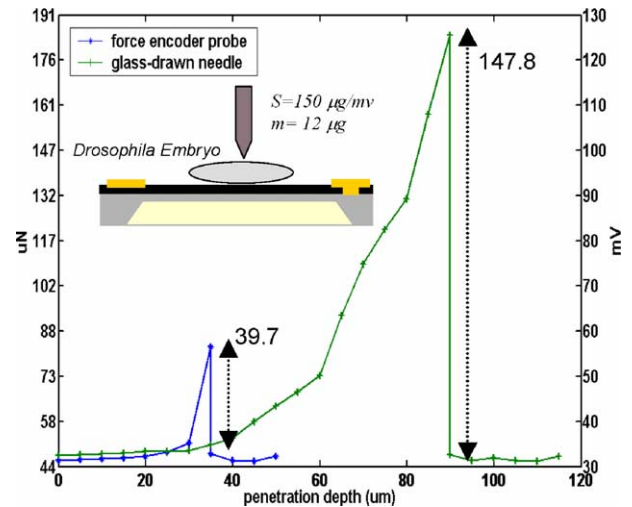


Fig. 6. DC calibration of the force encoder using SINTEF[®] piezoresistive microscale. Injections were performed on the posterior of a *Drosophila* embryo.

$\sim 150\ \mu\text{g}/\text{mV}$ to measure the injection force into *Drosophila* embryos. The injections were performed both with a traditional, commonly used drawn-glass needle with a typical $75\ \mu\text{m}$ diameter tip and with the silicon-nitride force encoder probe with a $30\ \mu\text{m}$ tip. The calibration set-up is shown in Fig. 6. The MEMS probe requires $\sim 40\ \mu\text{N}$ to penetrate the newly hatched embryo.¹ This is about four times less than the force needed for penetration with the conventional glass needle. In addition, the nitride probe needs a shorter traveling distance to reach penetration. Dynamic operation of the MEMS injector by off-chip piezoelectric actuation [10] is expected to further improve injection speed and cause less damage to the embryo.

The spring constant k of a force encoder ($W = 8\ \mu\text{m}$, $L = 10\ \mu\text{m}$) was measured using the same set-up. The measured value was $1.85\ \text{N}/\text{m}$ ($\pm 8.65\%$), in reasonable agreement with the simulation results. The discrepancy is assumed to be due to over-etching of the springs supporting the movable upper grating.

Fig. 7 shows the measurement set-up for the integrated force sensor. The sensor was illuminated by a HeNe laser ($633\ \text{nm}/4\ \text{mW}$) with spot sizes ranging from 60 to $160\ \mu\text{m}$. The power in the first-order diffracted mode is measured with a photodiode (embedded in a Coherent[®] Beam-View Analyzer) placed $5\ \text{cm}$ from the force encoder. Spatial filtering was performed to minimize the crosstalk

¹ *Drosophila* embryos 50 min after hatching are dechlorinated in 60% bleach for 1.5 min and then rinsed thoroughly with water ($20\ ^\circ\text{C}$). Properly staged embryos are selected and desiccated for 15 min in a sealed glass jar containing calcium sulfate (CaSO_4) desiccant. Finally, embryos are covered in Halocarbon 700 oil (Aqua-Air Industries Inc., Harvey, LA) and ready for injection.

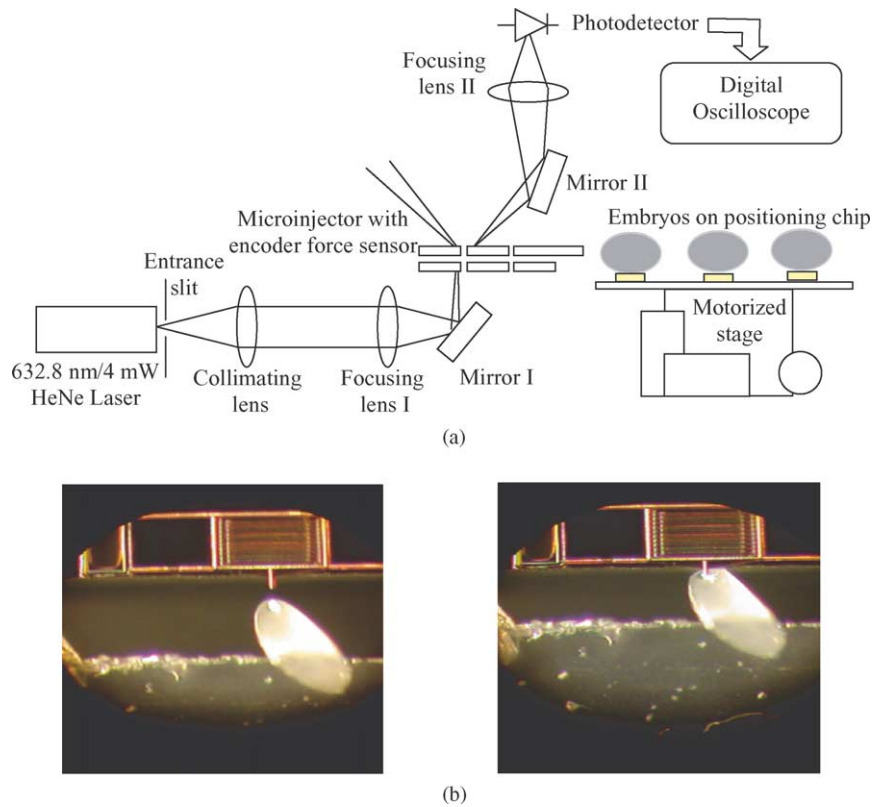


Fig. 7. (a) Set-up for injection force sensing measurement. The microinjector is held fixed while the embryos are moved by a motorized stage. (b) Close-up views of injection into *Drosophila* embryos.

between diffraction orders. Fig. 8 shows the measured power of the first diffraction mode as a function of absolute displacement of the injector. This displacement includes both the relative displacement of the gratings and the displacement of the embryo membrane. The grating

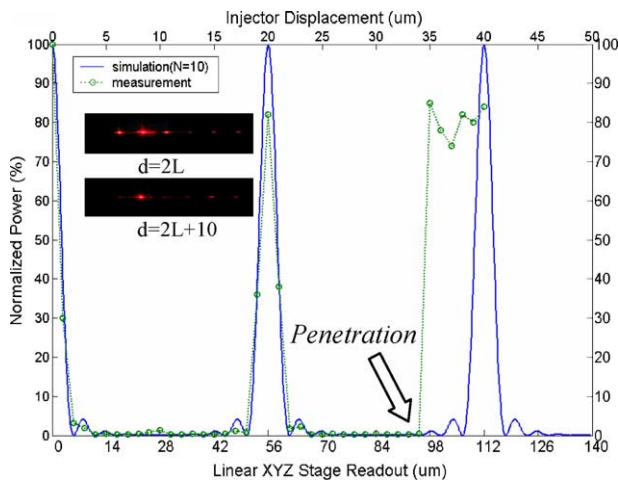


Fig. 8. First diffraction mode power vs. injector displacement of a force encoder with $N = 10$, $L = 10 \mu\text{m}$ and $K_y = 1.85 \text{ N/m}$. The measured injection force measured: $F = 63 \mu\text{N}$. The inserts show typical diffraction patterns at penetration depths of $d = 2L$ and $d = 2L + 10$.

displacement can be found from the known $20 \mu\text{m}$ period of the diffraction response. Using this calibration and a spring constant of 1.85 N/m , we find an injection force of $63 \mu\text{N}$. This assumes that the membrane behaves like a linear spring under small deformation. The sensor as tested here has a significant sensitivity around $d = 2L$, but, since its output is ambiguous around the displacement where penetration takes place, it cannot be used to verify the assumption that the membrane deformation is linear in the force. The solution is provided by illuminating fewer periods of the force encoder. As shown in Fig. 9, the same force sensor illuminated by a laser spot size of $60 \mu\text{m}$ ($N = 3$), has an improved dynamic range (45% increase), at the cost of lower sensitivity ($18\%/\mu\text{m}$ reduction). In this case, the diffraction is not ambiguous around the penetration displacement, so both the penetration force ($48 \mu\text{N}$) and the embryo membrane deformation ($57 \mu\text{m}$) at penetration can be determined. In a series of experiments, we found an average penetration force of $52.5 \mu\text{N}$ ($\pm 13.2\%$) and an embryo deformation of $58 \mu\text{m}$ ($\pm 5.2\%$). The measurements are in reasonable agreement with the piezoresistive-scale calibration data, demonstrating that the optical MEMS encoder force sensor has sufficient sensitivity and dynamic range for monitoring penetration and injection force dynamics in *Drosophila* embryos.

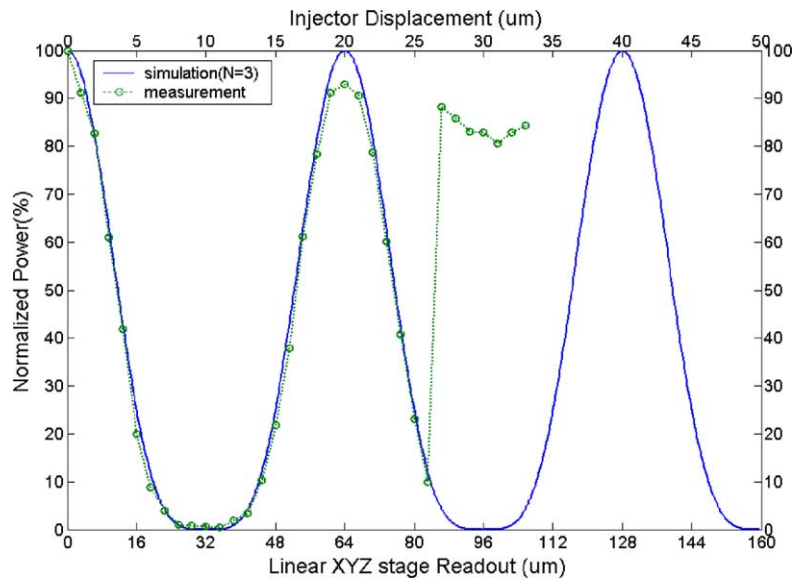


Fig. 9. Force sensing with large dynamic range with $N = 3$, $L = 10 \mu\text{m}$ and $K_y = 1.85 \text{ N/m}$. The measured embryo injection force is $F = 48 \mu\text{N}$.

5. Conclusions

We present an integrated optical-encoder force sensor with configurable sensitivity and sufficient dynamic range for monitoring penetration and injection force in *Drosophila* embryos. The encoder is based on transmission phase gratings to optimize optical throughput and it is designed to have low sensitivity to rotation and cross axis translation. Tunability of the sensor can be achieved by either using arrays of integrated optical encoders with various pitch periods or varying the size of the optical illumination window on a fixed period encoder. The periodicity of the encoder gratings can be used for sensor self-calibration. These advantages of the integrated optical MEMS encoder force sensor make it a versatile tool for studying and controlling cell-membrane penetration, and give it the potential to facilitate development of microinjection and microsurgery instrumentation for a wide range of applications.

Acknowledgements

This work was funded by the DARPA [Bio:Info:Micro] program (MDA972-00-1-0032). The authors wish to thank Professor Calvin F. Quate for helpful discussions and the technical staff at the National Nanofabrication Users Network (NNUN) facilities and Edward L. Ginzton Lab at Stanford University for their support.

References

- [1] M.P. Scott, Hox genes, *Nat. Genet.* 15 (1997) 117–118.
- [2] S. Zappe, X.J. Zhang, R.W. Bernstein, E.M. Furlong, M. Fish, M.P. Scott, O. Solgaard, Micromachined hollow needle with integrated

pressure sensors for precise, calibrated injection into cells and embryos. In: *Proceedings of the Sixth International Symposium on Micro Total Analysis System (μTAS)*, vol. 2, 2002, pp. 793–795.

- [3] J. Guild, *Diffraction Gratings as Measuring Scales*, Oxford University Press, Oxford, UK, 1960.
- [4] S.R. Manalis, S.C. Minne, A. Atalar, C.F. Quate, Interdigital cantilevers for atomic force microscopy, *Appl. Phys. Lett.* 69 (25) (1996) 3944–3946.
- [5] N. Hall, F.L. Degertekin, Integrated optical interferometric detection method for micromachined capacitive acoustic transducers, *Appl. Phys. Lett.* 80 (2002) 3859–3861.
- [6] N. Loh, M.A. Schmidt, S.R. Manalis, Sub-10 cm^3 interferometric accelerometer with nano- g resolution, *J. Microelectromech. Syst.* 11 (3) (2002) 182–187.
- [7] R. Sawada, E. Higurashi, O. Ohguchi, Monolithically integrated micro-encoder, *Appl. Opt.* 38 (1999) 1746–1751.
- [8] K. Hane, T. Endo, M. Ishimori, Y. Ito, Y. Sasaki, Integration of grating-image-type encoder using Si micromachining, *Sens. Actuators A: Physical* 97–98 (2002) 139–146.
- [9] J.W. Goodman, *Introduction to Fourier Optics*, 2nd ed., McGraw-Hill Science/Engineering/Math, 1996.
- [10] A. Lal, R.M. White, Micromachined silicon needle for ultrasonic surgery, *Proceedings of the IEEE Ultrasonics Symposium*, 1995, pp. 1593–1596.

Biographies

X.J. Zhang received his BSc degree in precision electronic instrumentation and biomedical engineering from Shanghai Jiao Tong University, China in 1995 and his MSc degree in electrical engineering from University of Maine, Orono in 1998. His industrial experience includes working at Hewlett-Packard (later, Agilent Technologies) on the design of parallel optical interconnects and technical consulting for Cisco Systems on the evaluation of IEEE802.3ae 10Gb/s optical transceivers. He is currently a PhD candidate in electrical engineering at Stanford University. His dissertation research includes diffractive optical microelectromechanical systems (Optical MEMS) and Bio-MEMS design, fabrication and characterization, with focus on developing integrated microphotonic sensing interface for in vivo single cell and embryo manipulation, force microscopy and near-field imaging.

S. Zappe received his Diploma degree in electrical engineering from the Berlin University of Technology, Germany, in 1996. From 1996 until 2001 he worked as a PhD student at the Microsensor and Actuator Center at the Berlin University of Technology. In February 2001, he joined the Stanford Microphotonics Laboratory at Stanford University, CA, USA as a Postdoctoral Researcher. His research activities include microfluidic systems for cell- and embryo-handling, sorting and micro-injection; biology of fruit fly development; gene silencing by means of RNAi (RNA interference); micro-orifices for DNA shearing; microfluidic systems-based re-usable arrays for DNA sequencing; integration of active and passive optical components into microsystems.

R.W. Bernstein received his doctoral degree in physical electronics in 1990 from the Norwegian Institute of Technology (NTH) in Trondheim, Norway. He is now Research Director at SINTEF Electronics and Cybernetics, Department of Microsystems. He started at SINTEF as a Senior Scientist from 1992 and became Research Director in 1996. Before that he was employed as a Research Scientist at Norwegian Telecom Research from 1990 to 1992. He was Associate Professor II at the University of Tromsø from 1996 to 2001. Bernstein was on leave from SINTEF as a visiting Scholar at Ginzton Laboratory, Stanford University, CA, USA in 2001–2002. Ralph W. Bernstein's fields of expertise are within III–V semiconductor technology, microsystem technology (MST) and MEMS design. His recent research interests have focused on BioMEMS for high throughput injection of biological material into embryos and cells. He is a member of the technical committee for the European EUREKA-program, EURIMUS, and is an evaluator within the thematic area IST of the 6th EU framework program.

O. Sahin received his BSc degree in electrical engineering from Bilkent University, Ankara, Turkey in 2001 and MSc degree from Stanford University, CA in electrical engineering in 2003. He is currently working towards his PhD degree in electrical engineering at Stanford University, CA. His research interests include sensors based on nanomechanics and nanooptics and manipulation of cells within microfluidic systems. He is a student member of IEEE.

C.-C. Chen received his BSc degree in mechanical engineering from National Taiwan University, Taiwan, in 1994 and his PhD degree in power mechanical engineering from National Tsing Hua University, Taiwan in 1999. He worked as an engineer with the Microsystem Technology Division, Electronics Research and Service Organization (ERSO) of the Industrial Technology Research Institute (ITRI), Taiwan, between 2000 and 2002. He is currently a postdoctoral researcher in Stanford

University and is conducting his research at E.L. Ginzton Labs. His current research focuses on microfluidic device design, simulation, fabrication and characterization for several applications including cell sorting, fluid dispensing, micro-droplet injecting and device cooling, for which he holds three related patents.

M. Fish received his BSc degree in biology from San Jose State University, San Jose, CA, in May 1991 and his MSc degree in molecular biology from San Jose State University in May 1999. He is currently employed by the Howard Hughes Medical Institute, working at Stanford University, Stanford, CA in the Department of Developmental Biology. His research work focuses on the function of a novel, developmentally regulated gene in *Drosophila melanogaster*.

M.P. Scott received his BS and PhD degrees in biology from MIT. He did postdoctoral research at Indiana University and then joined the faculty at the University of Colorado at Boulder. In 1983, he moved to Stanford University School of Medicine where he is now Professor of Developmental Biology and of Genetics. He has published more than 130 papers and three patents. His research areas are developmental genetics and cancer research, particularly the roles of signaling systems and transcriptional regulation in embryonic development. His research employs genetics, genomics, cell biology, and molecular biology in exploring how cells acquire their fates and are patterned. He is an editor of Current Opinion in Genetics and Development and of the Proceedings of the National Academy of Sciences. He is a past president of the Society for Developmental Biology, a member of the American Academy of Arts and Sciences, and a member of the National Academy of Sciences. He is presently chairing Stanford's Bio-X program, which is designed to accelerate the coming together of engineering, physics, and chemistry with biology and medicine.

O. Solgaard received the BS degree in electrical engineering from the Norwegian Institute of Technology and his MS and PhD degrees in electrical engineering from Stanford University, California. He held a post doctoral position at the University of California at Berkeley, and an assistant professorship at the University of California at Davis, before joining the faculty of the Department of Electrical Engineering at Stanford University in 1999. His research interests are optical communication and measurements with an emphasis on semiconductor fabrication and MEMS technology applied to optical devices and systems. He has authored more than 100 technical publications, and holds 13 patents. He is a co-founder of Silicon Light Machines, Sunnyvale, CA, and an active consultant in the MEMS industry.